Materials Science in Semiconductor Processing ▮ (▮▮▮▮) ▮▮▮–▮▮▮

Contents lists available at ScienceDirect

Materials Science in Semiconductor Processing

journal homepage: www.elsevier.com/locate/mssp

Sonosynthesis of microstructures array for semiconductor photovoltaics

R.K. Savkina [a,*], A.B. Smirnov [a,*], T. Kryshtab [b], A. Kryvko [c]

[a] V. Lashkaryov Institute of Semiconductor Physics at NAS of Ukraine, pr. Nauki 41, C.P., 03028 Kiev, Ukraine
[b] Instituto Politécnico Nacional – ESFM, Department of Physics, Av. IPN, Ed. 9, U.P.A.L.M., C.P., 07738 Mexico D.F., Mexico
[c] Instituto Politécnico Nacional – ESIME Zacatenco, Av. IPN, Ed. Z4, U.P.A.L.M., 07738 Mexico D.F., Mexico

ARTICLE INFO

Keywords:
Silicon
Strain engineering
Ultrasonic cavitation
Dendritic structure

ABSTRACT

The properties of the silicon samples subjected to cavitation impacts have been studied. It was shown that high-intensity (15 W/cm^2) and high-frequency (1–6 MHz) sonication of silicon samples in the liquid nitrogen induces changes of the physical, chemical, and structural properties of semiconductor surface. Optical, atomic force and scanning electron microscopy techniques as well as energy dispersive X-ray spectroscopy, X-ray diffraction and photoresponse spectroscopy were used. The experimental study demonstrates the microstructure formation as well as a change of the chemical composition at the silicon surface. It was found that a significant rise in value and expansion of the spectral range of photosensitivity take place after cavitation treatment. The photoresponse of about 2.0 eV can be connected with the formation of Si-rich SiN_x compound inside the ultrasonically structured region of Si. The obtained value of the refractive index confirms this assumption.

1. Introduction

Structuring of semiconductor surfaces is important in many branches of science and technology [1]. Such surface properties as roughness, light reflectivity, chemical activity, and biocompatibility have a potential use especially in electronics and medicine. For example, standard solar cell fabrication technique uses silicon wafers with textured surfaces, since the surface texturing is a well-established strategy for reducing reflection. Surface structuring is also applied in MEMS (micro-electromechanical systems) [2]. Thanks to the development of such booster technologies as reactive ion etching, isotropic etching, plasma ashing/cleaning the manufacturing of all silicon devices based on the scaling law became possible [3]. At the same time solid surfaces can develop a wide range of topological features upon bombardment with ions as well as under irradiation by laser pulses with femto- and picosecond duration. Nowadays, ultrasound is used extensively in mechanical engineering for bonding and manipulation in micro-machines, for cleaning in electronic engineering and medical/pharmaceutical industries, for nondestructive control and measurement, for health diagnosis, food treatment, etc. [4]. Extreme conditions of the ultrasonic cavitation such as local temperature and the pressure [5] are widely used in chemistry, as for example to synthesize nano-materials [6], to enhance the electrochemical reactions and to modify the surface properties of electrodes [7], as well as to generate the novel materials in a liquid medium [8].

In the previous work, we have shown that the exposure of semiconductor substrate to megasonic cavitation leads to the surface structuring [9,10]. It was revealed that the characteristic dimension of the peculiarities on the semiconductor surface depended on the exposure parameters

* Corresponding authors. Tel.: +38 044 525 5461; fax: +38 044 525 6296.
E-mail addresses: r_savkina@lycos.com (R.K. Savkina), alex_tenet@isp.kiev.ua (A.B. Smirnov).

http://dx.doi.org/10.1016/j.mssp.2015.02.066
1369-8001/

and can be controlled (from micron- to nano-scale dimension) by the regulation of the acoustic frequency. In this investigation, we demonstrate that topological features induced by sonication on the semiconductor surface can be useful for the photovoltaic application.

2. Experimental section

2.1. Materials

Boron-doped *p*-type silicon (wafers grown by the liquid-encapsulated Czochralski method, with diameter about 76.2-mm, one-side polished), with a (100) surface crystallographic orientation, were used in this study. Samples were cut into 5 mm × 5 mm squares to fit the sample holder used for sonication experiments. Before the investigation all samples were cleaned for 10 min in ethanol and then in ddH_2O (water for analytical laboratory use, ISO 3696:1987). The initial surface was found to be totally flat, devoid of defects, with a measured roughness lower than 1 nm. The roughness was determined by atomic force microscopy (AFM) on a few randomly chosen areas of $40 \times 40\ \mu m^2$. X-ray diffraction (XRD) patterns from the initial samples besides the Si 400 diffraction peak reveal higher intensity background in the range of $2\theta = 20–30^\circ$ that denotes the existence on the Si substrate surface of amorphous thin film, obviously from the amorphous native silicon oxides, as was observed in [10]. This layer was not removed as it is going to disappear during the process of sonication, since the modified region is entirely below the original surface.

2.2. Sonication and post-treatment annealing

In typical experiments, the Si samples were sonicated in cryogenic liquid such as liquid nitrogen (LN). For cavitation activation, a homemade megasonics (1–6 MHz) system with focused energy resonator described elsewhere [9] was used. Semiconductor target was placed inside the acoustically driven copper cell filled with technical liquid nitrogen, where the cavitation processing was initiated. The maximal value of the acoustic intensity was about ~15 W/cm^2 in the focus of the acoustic system. Sonication were performed at constant temperature (80 K) using a cryostat system. Post thermal annealing was carried out in the atmospheric ambient at 980 °C for 1 h.

2.3. Characterization

All processed surfaces were examined after fixed cavitation intervals using optical and atomic force microscopy. Scanning electron microscopy (SEM) characterization was realized using JSM-6490 microscope supplemented by energy dispersive X-ray analysis (EDAX). Operating conditions for SEM and EDAX were the same. A standard procedure of photoresponse spectroscopy was employed before and after the sonication. The structural characterization of the silicon samples was carried out by XRD in the standard symmetric reflection geometry using CuKα radiation. XRD rocking curves measured using the ω-2θ scan for the samples investigated before and after sonication were obtained by a Triple-axis X-ray PANalytical X'Pert Pro diffractometer. The CuKα1 radiation with a wavelength of 0.15418 nm was separated out using a four-bounce (440) Ge monochromator. The optical characteristics of the typical annealed sample were studied by ellipsometry. The measurements were performed using a laser ($\lambda = 632.8$ nm) photoelectric compensation null ellipsometer (LEF 3G-1). The ellipsometric parameters Δ and ψ were determined from the results of multi-angle measurements in a range of incidence angle $\phi = 50–75^\circ$.

3. Results

It was found that the sonication of the silicon samples has resulted in the essential change of the physical and structural properties of semiconductor surface. First of all, the sonication has resulted in the silicon surface structuring as well as in a significant rise of the silicon photosensitivity.

3.1. Surface morphology and elemental composition

In the previous work we observed that the characteristic dimension of the structures on the semiconductor surface depends on the exposure parameters (duration, acoustic power) and can be controlled by the regulation of the acoustic frequency [9]. In particular, a dendrite-like micron-scale array formation inside the ultrasonically structured region was found. In this investigation, morphology of the structured surface was investigated using different techniques. Optical microscopy revealed the growth of dendritic crystal inside the structured region of Si sample during sonication at the maximum value of acoustic intensity in the LN at 1–3 MHz (Fig. 1a). The increase of processing time results in the appearance of the features with crystal symmetry as shown in Fig. 1b. Fig. 1c illustrates the changes in the silicon surface after the post-sonication annealing.

Fig. 2 illustrates SEM and AFM images of ultrasonically structured regions with the dendrite-like structures of silicon sample sonicated in the liquid nitrogen before annealing. The height of typical dendrite-like structures measured using AFM was about 160 – 200 nm (see Fig. 2b). SEM characterization supplemented with EDAX shows that both surface morphology and the elemental composition of the silicon surface undergo dramatic changes at a small scale under sonication. The chemical composition of the samples was studied on a numerous randomly chosen areas of $5 \times 5\ \mu m^2$ as shown in Fig. 2a. EDAX shows that together with the peaks corresponding to Si atoms appeared the peaks corresponding to the following elements: O, Na, K, Ca and Cl (see Table 1). In our previous investigation we found an inhomogeneous incorporation of the nitrogen atom into the GaAs substrate exposed to the acoustic cavitation in liquid nitrogen [9]. At the same time, the nitrogen atoms on the silicon surface have not been observed by EDAX. Ultrasonically structured regions with the dendrite-like structures have a silicon nature, contain a number of alkali metals (region 2, Fig. 2a, Table 1) and are surrounded with the oxidized surface (region 3, Fig. 2a, Table 1).

Please cite this article as: R.K. Savkina, et al., Materials Science in Semiconductor Processing (2015), http://dx.doi.org/10.1016/j.mssp.2015.02.066

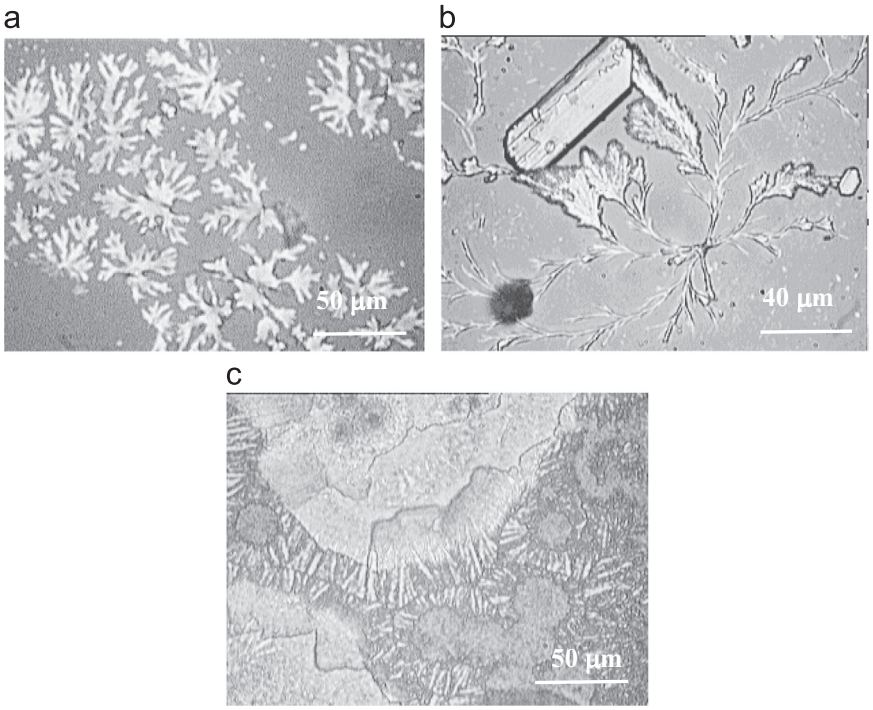

Fig. 1. Optical micrographs of the typical Si sample exposed to the acoustic cavitation in liquid nitrogen at 3 MHz during (a) 15 min and (b) 30 min, (c) – the same sample after annealing during one hour at 980 °C.

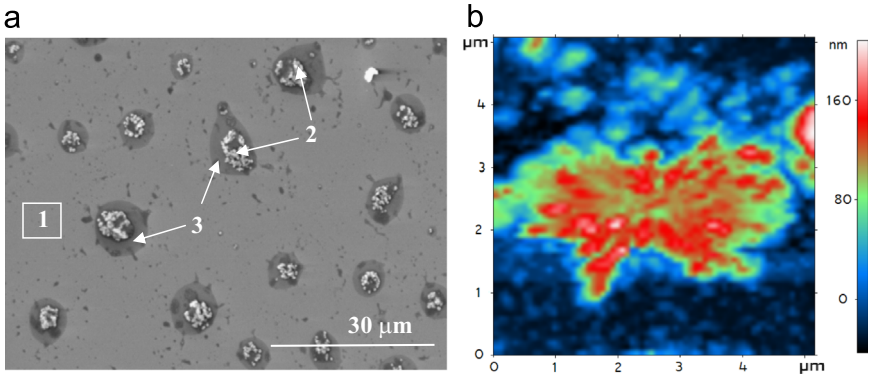

Fig. 2. SEM and AFM images of ultrasonically structured regions with the dendrite-like structures before annealing: (a) – electron micrograph (7 kV, 2000 ×) of silicon sample sonicated in the liquid nitrogen, (b) – AFM image of the dendrite-like object.

Table 1
Weight percent (wt%) of the elements determined by EDAX technique for silicon sample sonicated in LN. Regions 1–3 are depicted on the Fig. 2a.

Element	Region 1	Region 2			Region 3
OKα	–	2.09	2.01	2.19	0.65
NaKα	–	0.71	0.62	0.83	–
SiKα	100	93.24	94.48	95.11	99.35
ClKα	–	2.27	1.51	1.33	–
KKα	–	2.09	1.19	0.54	–
CaKα	–	–	0.19	–	–

It should be noted that since the samples were cleaned with double-distilled water, a source of impurities is rather technical nitrogen (or experimental cell) than ddH_2O. Moreover, we found not only a surprising amount of impurities on the silicon surface, but also compounds having a crystal structure such as $Na_2Ca_3(Si_3O_{10})$ and $CaSiO_3$ (see Ref. [10]). Last compound is important in the ceramics and exhibits a good bioactivity and biocompatibility. Obviously favorable conditions to sonochemical synthesis of silicates are created in the experimental cell. Our future efforts will be made just in this direction.

3.2. Surface photovoltage spectra

Untreated Si samples exhibit very low level of the photosensitivity. The initial spectrum consists of a selective peak with the spectral position of the 'red' boundary, which corresponds with the silicon band gap $E_g = 1.158$ eV

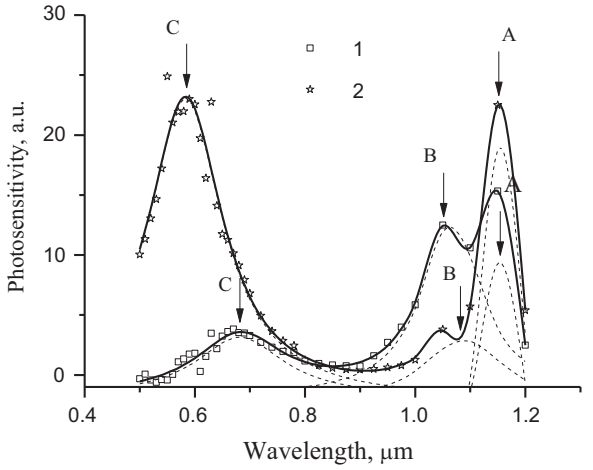

Fig. 3. Surface photovoltage spectra of the typical silicon sample subjected to the acoustic cavitation during 15 min (curve 1) and 30 min (curve 2) in liquid nitrogen at 3 MHz after annealing during 1 h at 980 °C. The measured value of the photovoltage was about 30 μV at light power density ~0.01 W mm^{-2} after treatment. The dots indicate the experimental data and the solid lines present the results of the fitting procedure. The thin-dash lines show approximation by the Lorentzian model.

Table 2
Peak positions of the surface photovoltage spectra presented in Fig. 3.

Peak position	A (eV)	B (eV)	C (eV)
After 15 min of sonication	1.07	1.17	1.82
After 30 min of sonication	1.07	1.15	2.13

(300 K). After sonication, significant rise in value of the photosensitivity was found. Moreover, the annealing for one hour at 980 °C resulted in the expansion of the spectral range of photosensitivity towards the visible region >2 eV. Fig. 3 illustrates surface photovoltage spectra of the typical silicon sample after sonication and post thermal annealing. It is seen abrupt increase of photoresponse at about 1.2 eV (peak A) corresponding to the silicon band gap E_g=1.158 eV (300 K). The spectra show also a peak in the photoresponse at about 1.07 eV. We suppose that the presence of this peak indicates the strain-induced narrowing of silicon band gap [11]. Photoconductive response indicates the presence of a wide-gap feature (see Fig. 3, peak C), which seems to occur after annealing of the samples investigated. Moreover, the processing time increase results in the short-wavelength shift (from 1.8 eV to 2.1 eV) and in the increase of the absolute value of this peak. We believe that the wide-gap peak is associated with a new compound formation on the silicon surface. The peak positions were obtained from the corresponding approximation by the Lorentz curves fitted to the experimental ones (see Fig. 3, dash lines).

3.3. Ellipsometry

The optical characteristics of the annealed sample were studied by ellipsometry. The optical parameters were

Table 3
Optical characteristics of a typical annealed silicon sample subjected to the acoustic cavitation.

Layers	*n*	*k*	*d*
Substrate Si	3.88	0.029	semi-infinity
First layer	3.12	0.026	500–900 nm
Second layer	1.43–1.48	→	130 nm

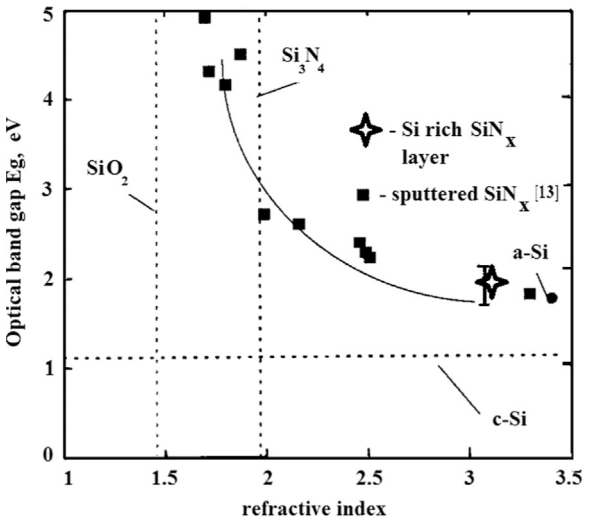

Fig. 4. The variation of the refractive index for SiN_x films with different compositions from amorphous silicon (a-Si) to nearly stoichiometric (Si_3N_4) from Ref. [13]. The "star" marks the parameters n=3.12 and E_g~2 eV obtained in our investigation.

calculated within the framework of the formation of the complex optical system with two transition layers after cavitation treatment and annealing. The values of the extinction coefficient k, the refractive index n and the thicknesses of layers are presented in the Table 3. According to the refractive index database [12] the first layer on the substrate may be associated with the formation of Si-rich SiN_x compound. Although EDAX did not reveal the presence of nitrogen atoms on the Si surface after treatment, which can be connected with different reasons, the probability of their incorporation is very high as treatment was carried out in liquid nitrogen. The second (top) layer has optical parameters, which are close to SiO_2 compound. To confirm our assumptions we can refer to the paper [13], which illustrates the correspondence between the values of the optical band gap and refractive index of sputtered SiN_x films with different compositions (see Fig. 4). The parameters of n=3.12 and E_g~2 eV, obtained in our investigation, are marked with the "star" and demonstrate a good agreement with the data from paper [13]. Considering this result it can be supposed, that layer with refractive index ~3.12 (Table 3) demonstrates the photoresponse at about 2.0 eV (photovoltage peak C, see Fig. 3 and Table 2). A more precise definition of the layers origin would require an additional research.

Please cite this article as: R.K. Savkina, et al., Materials Science in Semiconductor Processing (2015), http://dx.doi.org/10.1016/j.mssp.2015.02.066

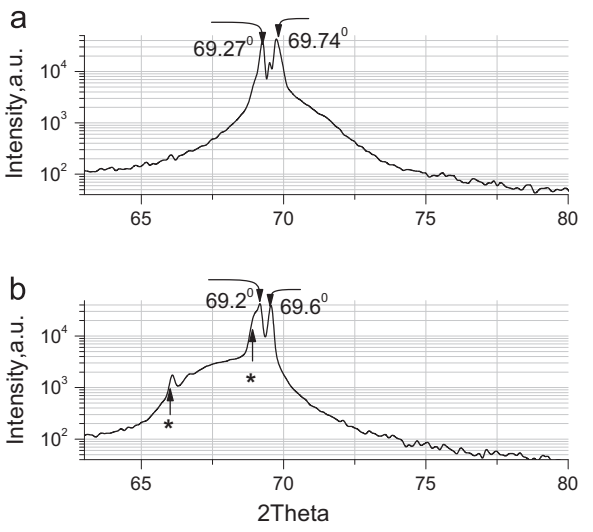

Fig. 5. XRD peaks for a typical Si sample after sonication (a) and post-sonication annealing (b). The additional peaks marked by asterisks (*), can be attributed to the formation of the new phase after sonication and post-sonication annealing.

3.4. X-ray diffraction

The XRD peak from Si (400) wafer after the cavitation treatment is shown in Fig. 5a. Splitting of this curve was observed. An intense peak at $2\theta=69.27^\circ$ corresponding to (400) reflection for silicon and an intense peak at $2\theta=69.74^\circ$ were detected. Moreover, the peak with intensity $0.5I_{400}$ is observed between the mentioned peaks. This splitting is probably related to the reflection from the surface layer formed at cavitation treatment and silicon wafer without abrupt interface. After post-sonication annealing the main peak splitting remained, but became smaller (Fig. 5b) that can be connected with the partial interdiffusion of the additional element in the structured region (Table 1) and silicon wafer. At the same time, appearance of the additional peaks (marked by asterisks, in Fig. 5b) at the low angle side of the main peaks can be attributed to the formation of the new phase on the silicon surface in ultrasonically structured regions after the annealing. Unfortunately, we could not identify them yet.

X-ray rocking curves for the samples investigated before and after sonication are shown in Fig. 6. Rocking curve broadened out and shifted towards the larger angle after cavitation processing with respect to the rocking curve for initial state that indicate the appearance of compressive strains in perpendicular direction to the surface of silicon samples (Fig. 6). This result correlates with splitting of the Si (400) diffraction peak (Fig. 5) since it is well known that the presence of coupled layer on the crystal surface with different structure parameters induces the lattice strains.

4. Discussions

Our experimental study demonstrates the microstructures formation as well as a change of the chemical composition up to the new phase formation on the silicon surface after the cavitation processing. Besides, the XRD investigation pointed to strains in the silicon lattice induced by the cavitation effect. It is obvious that an essential rise of the photosensitivity of the semiconductor wafer have been ascribed to the observed phenomena.

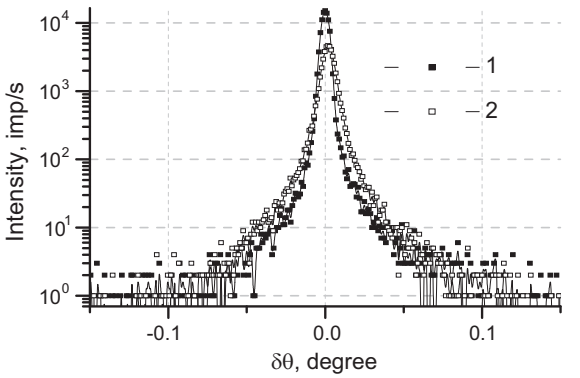

Fig. 6. X-ray rocking curves for a typical sample in initial state (1) and after cavitation treatment (2).

As we know, the photosensitivity of the semiconductor crystal is characterized by the photocurrent, which is proportional to the products of the mobility (μ) and lifetime (τ) for electrons and holes as $I_{PC}\sim(\mu\tau)_e+(\mu\tau)_h$. A known phenomenon of silicon wafer gettering at the cavitation impact [14] can result in the decrease of the rate of recombination through an energy state created within the band gap by a localized state. As a result the increase of carrier lifetime (τ) and diffusion length take place. On the other hand, strains have been introduced into Si technology as a mean of enhanced charge carrier mobility [15]. Finally, structuring of the surface is a known method to change the optical parameters and as a consequence to increase the efficiency of silicon solar cells. Thus, we think that the photosensitivity rise after sonication can be connected with the silicon surface microstructuring, gettering of the silicon wafer as well as modification of the band structure due to the cavitation processing.

It is also necessary to focus on the features of the interaction between cavitating liquid and semiconductor target, resulting in the phenomena described. It is well known that ultrasound passing through a liquid causes thermal agitation, which in turn gives rise to the formation of superheated vapor bubbles. Every one of these bubbles is asymmetrically imploded with the ejection of micro-jets of solvent at speeds of up to several hundred m/s. The bubble temperature reaches thousands of degrees Kelvin during collapse, pressure equals several hundreds of MPa, and heating and cooling rates are above 10^{10} K/sec [5].

On the basis of various theoretical studies and experimental data on cavitation-surface interaction, it is possible to assert that the micro-jet impact is a general physical mechanism responsible for the effect of cavitation near solid surface. The potential energy of an expanded bubble is converted into the kinetic energy of a liquid jet that transfers it to the substrate atoms at the site of impact. Since we deal with multibubble cavitation in an acoustic field, the interaction between bubbles with formation of

Please cite this article as: R.K. Savkina, et al., Materials Science in Semiconductor Processing (2015), http://dx.doi.org/10.1016/j.mssp.2015.02.066

compact groups – clusters, is possible. These clusters are attracted by the surface [16] and a significant surface area exposed to the multiple jet impacts. It can be suggested that a high density of energy transferred to the substrate atoms from the jet impact results in a local melting of a shallow layer of the semiconductor around the impact spot. The formation of the rim around circular regions observed elsewhere [9] confirms this assumption. Moreover, dendrite formation inside ultrasonically structured region of Si can points to the melted silicon supercooling as a result of the solidification point shift due to high pressure pulses associated with a collapsing bubble.

5. Conclusions

High-intensity sonication of silicon samples in the liquid nitrogen was shown to induce changes in the physical and structural properties of semiconductor surface. For the first time, it was found the dendrite-like micron-scale array formation as well as a change of the chemical composition up to the new phase occurrence inside the ultrasonically structured region. XRD results in the coherent-scattering region point out to the compression of the structured layer. Cavitation treatment with post-annealing of Si samples leads to the formation of a complex optical system with two transition layers. Significant rise in value and expansion of the spectral range of photosensitivity take place after cavitation treatment. The photoresponse of about 2.0 eV can be connected with the formation of Si-rich SiN_x compound inside the ultrasonically structured region of Si. The obtained value of the refractive index confirms this assumption.

Observed phenomena can provide an efficient route of investigations devoted to silicon solar cells improvement. This work also contributes to the understanding of the mechanism involved during the cavitation at the solid – liquid interface following megasonic cavitation treatment.

Acknowledgments

Authors are grateful to Dr. A. Gudymenko for X-ray rocking curves measurements and to A. Evmenova for ellipsometry measurements.

References

[1] A. Górecka-Drzazga, Opt. Appl. 37 (2007) 341–357.
[2] MEMS: design and fabrication, in: Mohamed Gad-el-Hak (Ed.), The MEMS Handbook, CRC Press LLC, 2005.
[3] H. Abe, M. Yoneda, N. Fujiwara, Jpn. J. Appl. Phys. 47 (2008) 1435–1455, http://dx.doi.org/10.1143/JJAP.47.1435.
[4] R.K. Savkina, Recent Patents on Electrical & Electronic Engineering, 6, 2013, pp. 157–172.
[5] J.H. Bang, K. Suslick, Adv. Mater. 22 (2010) 1039–1059, http://dx.doi.org/10.1002/adma.200904093.
[6] H. Xu, B.W. Zeiger, K.S. Suslick, Chem. Soc. Rev. 42 (2013) 2555–2567 , http://dx.doi.org/10.1039/c2cs35282f.
[7] D.G. Shchukin, H. Mohwald, Phys. Chem. Chem. Phys. 8 (2006) 3496–3506.
[8] M. Ashokkumar, T. Mason, Sonochemistry, Kirk-Othmer Encyclopedia of Chemical Technology, 2007.
[9] R.K. Savkina, A.B. Smirnov, J. Phys. D: Appl. Phys. 43 (2010) 6. 425301.
[10] T.G. Kryshtab, R.K. Savkina, A.B. Smirnov, MRS Proc. 1534 (2013) A87–A92, http://dx.doi.org/10.1557/opl.2013.304.
[11] Ting-Kuo Kang, IEEE Electron Device Lett. 33 (2012) 770–772, http://dx.doi.org/10.1109/LED.2012.2191759.
[12] M.N. Polyanskiy. Refractive index database. Available at http://refractiveindex.info.
[13] M. Vetter, Thin Solid Films 337 (1999) 118–122.
[14] M. Virot, R. Pflieger, E.V. Skorb, J. Ravaux, T. Zemb, H. Mohwald, J. Phys. Chem. C 116 (2012) 15493–15499.
[15] F. Chen, Ch. Euaruksaku, Zh. Liu, F.J. Himpsel, F. Liu, M.G. Lagally, J. Phys.D:Appl.Phys 44 (2011) 8, http://dx.doi.org/10.1088/0022-3727/44/32/325107. 325107.
[16] R. Mettin, Bubble and Particle Dynamics in Acoustic Fields: Modern Trends and Applications, in: A.A. Doinikov (Ed.), Research Signpost, Kerala, India, 2005, pp. 1–36.